Electrochromic thin films of Zn-based MOF-74 nanocrystals facilely grown on flexible conducting substrates at room temperature

Cite as: APL Mater. 7, 081101 (2019); doi: 10.1063/1.5108948
Submitted: 4 May 2019 • Accepted: 12 July 2019 •
Published Online: 1 August 2019

Abhijeet K. Chaudhari, Barbara E. Souza, and Jin-Chong Tan[a)]

AFFILIATIONS

Multifunctional Materials and Composites (MMC) Laboratory, Department of Engineering Science, University of Oxford, Parks Road, Oxford OX1 1PJ, United Kingdom

Note: This paper is part of the special topic on Open Framework Materials for Energy Applications.
[a)]**Author to whom correspondence should be addressed:** jin-chong.tan@eng.ox.ac.uk

ABSTRACT

Electrochromic materials can reversibly switch color subject to the application of an externally applied electrical potential, making them useful for advanced applications such as smart windows, sensors, and electrochromic displays. To date, the development of electrochromic metal-organic frameworks (MOFs) is hampered by their insulating framework and nonredox active moieties. Herein, we demonstrate the use of the Guest@MOF concept to engineer electrochromic thin films, termed "DHTP@Zn-MOF-74," grown on a flexible PET polymer substrate coated with a transparent indium tin oxide conductor. This electrochromic film reversibly switches between the (transparent) colorless ⇄ magenta states, by employing a relatively low cyclic voltage of 0 V and −2.5 V, and is tested under a variable scan rate ranging from 50 mV/s up to 1 V/s. This study could open the door to the discovery of new Guest@MOF electrochromic systems with tunable properties for energy applications.

Inorganic-organic (hybrid) materials termed "metal-organic frameworks" or "MOFs" are open-framework compounds emerging as a promising class of materials for energy[1,2] and device[3–5] applications. One of the most attractive characteristics of MOFs is their periodic long-range ordering (i.e., crystalline structure) featuring functionally active voids or interconnected pores (channels) with vast tunability.[6] Notably, the MOF pores can act as a *host* structure to accommodate another functional *guest* molecule to yield a "Guest@MOF" composite system.[7] Because of the strong host-guest interactions resulting from the nanoscale pore confinement, novel guest-induced properties such as electronic conductivity,[8] energy/charge transfer,[9,10] and tunable optical properties[11] have recently been demonstrated in a number of Guest@MOF composites. The Guest@MOF concept[7] offers a unique prospect to engineer new properties distinctive from those of the host framework or the guest molecules considered in isolation.

Electrochromism refers to the phenomenon where reversible color changes occur via electrochemical oxidation-reduction of the electrochromic material subject to an applied electrical potential. Electrochromic materials have received much attention as they are useful for applications such as smart windows, sensors, and displays. The electrochromic effect is widely explored using inorganic materials such as Prussian blue and their analogs,[12,13] metal oxides such as WO_3 and V_2O_5,[14,15] organic molecules,[16] oligomers,[17] and polymers.[18] Right from the early 1960s, many patents have been filed by electronics companies for electrochromic displays and smart glass applications adopting the concept of electrochromism. Although MOFs have been an active topic of research for ~20 years, the electrochromic phenomenon of MOFs has rarely been explored until quite recently. This is because the majority of MOFs have insulating behavior and nonredox nature, thereby suppressing the development of this topic area. Representative examples available to date comprise a number of electrochromic MOFs with either naphthalenediimide-based ligands[19–21] or pyrene-based ligands[22] deposited as a thin film on fluorine-doped tin oxide (FTO) glass substrates for improved conductivity.

In this letter, we demonstrate a facile approach by integrating electrochemistry and dip coating techniques to grow a polycrystalline thin film of Zn-MOF-74 onto a transparent flexible substrate. Herein, we adopt the concept of Guest@MOF to confine redox-active guests within the 1-D pore channels of the Zn-MOF-74 host, thereby resulting in an electrochromic switchable material, termed "DHTP@Zn-MOF-74" [Fig. 1(a)]. The electrochromic film is deposited on a conducting indium tin oxide (ITO)-coated PET polymer substrate, offering bending flexibility and mechanical toughness not found in electrochromic MOF films typically grown on FTO-coated glass substrates.

Zn-MOF-74 is an example of the porous MOF structure that exhibits 1-D hexagonal channels, whose pore dimensions are 12.7 × 12.7 Å^2, as depicted in Fig. 1(a). Its pore configuration is ideal

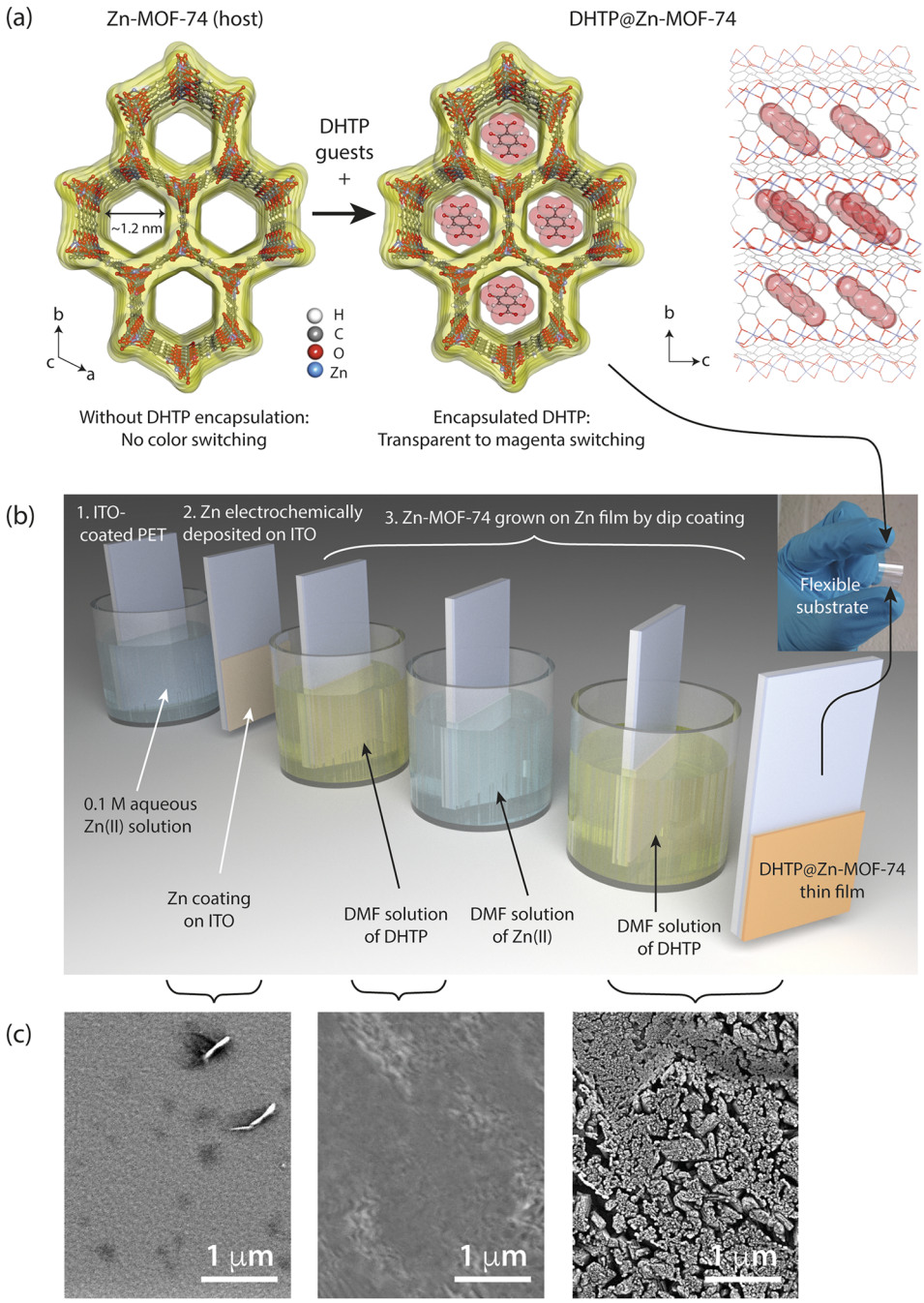

FIG. 1. (a) Schematic of the Zn-MOF-74 crystal structure showing the nano-sized 1-D pore channels oriented down the *c*-axis. These extended 1-D channels can be utilized to confine redox-active molecules (herein DHTP guests) to yield an electrochromic Guest@MOF composite. (b) The sequence of processing steps at room temperature to fabricate the thin film of DHTP@Zn-MOF-74 on a conductive ITO-coated PET polymer substrate. (c) FESEM micrographs of the thin film surface at particular stages of the fabrication process. Additional electron micrographs are shown in Figs. S3 and S4.

to confine redox-active "guest" molecules, herein the electroactive 2,5-dihydroxyterephthalic (DHTP) acid.[23] We chose the Zn-MOF-74 framework as a "host" framework considering the dynamic nature of plausible proton exchange sites conferred by its organic linker, which is also the DHTP acid. Its coordination environment has hydroxyl and carboxylic acid groups coordinated to the zinc metal centers to construct the extended structure illustrated in Fig. 1(a). Notably, the walls of the 1-D channels are replete with the zinc open metal sites[24,25] that could offer host-guest interactions with the nanoconfined guest species.

In this section, we describe the processing route to fabricate electrochromic thin films of DHTP@Zn-MOF-74 at room temperature. The steps involved are summarized in Fig. 1(b). We employed flexible ITO-coated PET (80 Ω/□) to develop transparent thin films of MOF-74 with encapsulated DHTP guests confined in the pore channels [Fig. 1(a)]. As the surface of the ITO-PET substrate is smooth and slippery, to enhance film adhesion, we electrochemically treat the ITO surface with an aqueous Zn(II) solution. Zn coating was deposited on the surface of the ITO in accordance with a reported procedure using the cyclic voltammetry (CV) technique.[26] CV was performed between −0.85 V and −1.055 V using a three-electrode configuration [see Fig. S1 in the supplementary material (SI)] where Ag/AgCl was used as the reference electrode, platinum as the counterelectrode, and ITO-coated PET as the working electrode immersed in a 0.1M aqueous solution of Zn(II) [prepared from zinc acetate, $Zn(OAc)_2$]. Five CV cycles were performed on the ITO

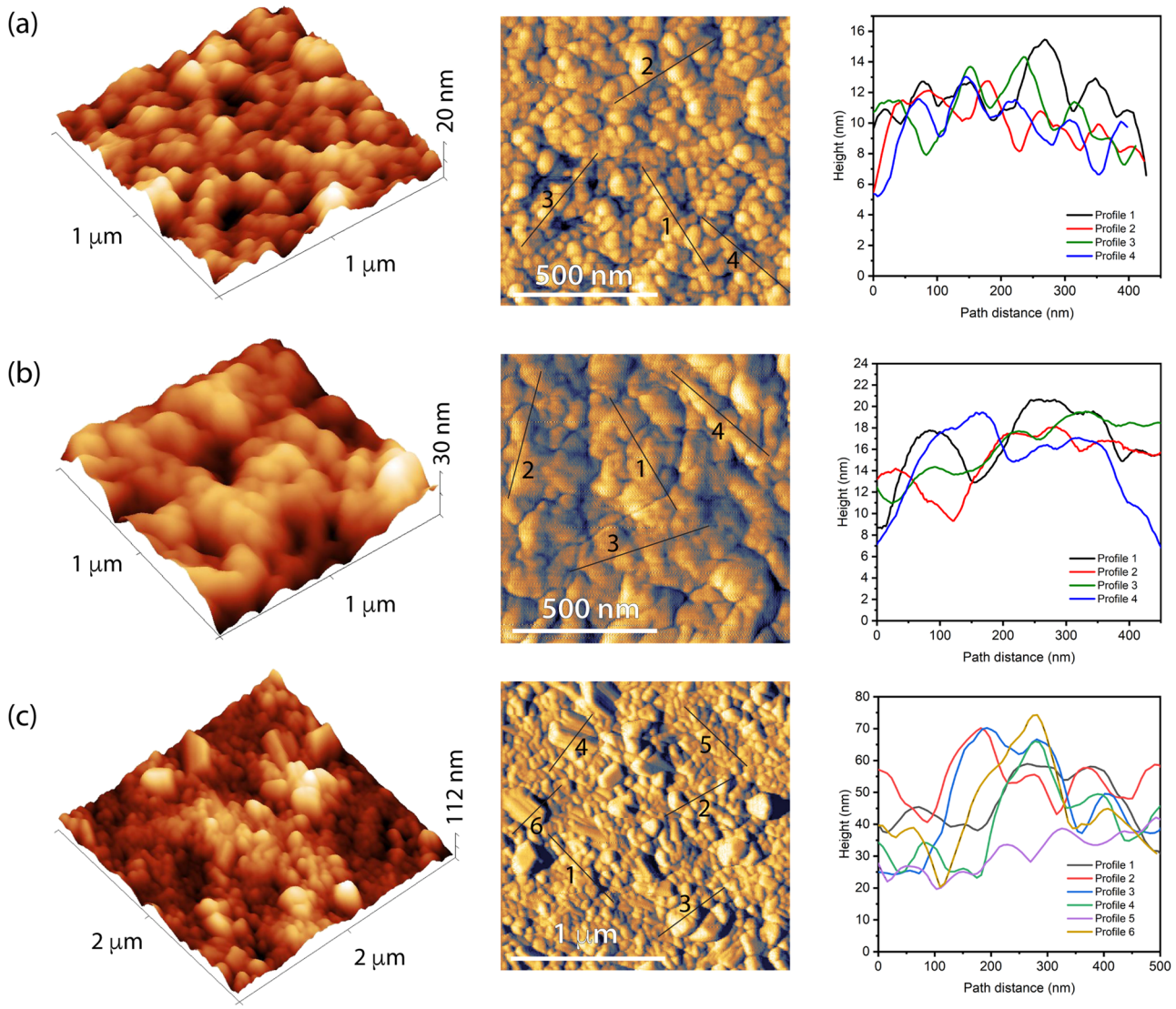

FIG. 2. AFM topography of the (a) ITO film on PET, (b) Zn polycrystals grown on the ITO, and (c) DHTP@Zn-MOF-74 polycrystalline film on the ITO-coated PET substrate. Additional AFM height profiles across the Zn to ITO interface and DHTP@Zn-MOF-74 to Zn interface are shown in Fig. S5.

coating to attain a Zn polycrystalline coating (Fig. S2 in the supplementary material), which was later immersed in a solution of DHTP in *N*, *N*-dimethylformamide (DMF) and Zn(II) in DMF solution sequentially. Specifically, 20 ml DMF solution of 1 mmol DHTP and 20 ml DMF solution of 2 mmol $Zn(OAc)_2$ were utilized for the dip coating process. First, the Zn-coated ITO-PET was dipped into the DHTP solution and then into the Zn(II) solution, and finally, it was immersed into the DHTP solution. Later, the substrate was allowed to air-dry at room temperature for 5–10 min and used directly for electrochromic studies.

The fine-scale surface morphology of the thin films was characterized using atomic force microscopy (AFM). Figure 2 shows the representative microstructures on the surface of the thin films obtained at different stages of the material fabrication process. It can be seen in Fig. 2(a) that the ITO film on the PET substrate consists of uniformly packed polycrystals, where the size of each ITO crystal was found to be ~30–50 nm. Figure 2(b) reveals that the Zn coating from CV deposition produced larger polycrystalline grains with an average grain size of ~50 nm. Finally, we found that the transparent film of DHTP@Zn-MOF-74 consists of relatively larger polycrystalline grains of ~50–100 nm. The powder X-ray diffraction (PXRD) pattern in Fig. S6 shows the crystallinity and structure of the Zn-MOF-74 (host) compound. PXRD peak broadening is attributed to the nanocrystalline morphology as evidenced in the AFM data. Thermogravimetric analysis (TGA) on DHTP@Zn-MOF-74 revealed the chemical formula of the compound as $[Zn_2(DHTP)(DMF)_2]_{12}$·DHTP, where ~3 wt. % of the DHTP guest molecule was found decomposing at about 300 °C before the host framework starts collapsing (see Fig. S7).

We have investigated the electrochromic behavior of the thin films by employing a three-electrode electrochemical cell setup (Fig. S1). We used Ag/AgCl as the reference electrode, platinum as the counterelectrode, and the DHTP@Zn-MOF-74 film as the test electrode. The electrolyte solution consisted of 0.1M tributylmethylammonium methyl sulfate conduction salt (MTBS) dissolved in DMF. Figure 3(a) shows a representative cyclic voltammetry (CV) test result by employing a scan rate of 50 mV/s: from 0 V decreasing to −2.5 V and rising back up to 0 V. The color changes exhibited by the thin film as a function of the applied voltage are presented in Fig. 3(b). The current density (mA/cm^2) was determined from the measured current normalized to the immersed area of the film in the electrolyte, corresponding to the sample region switching between transparent and magenta states.

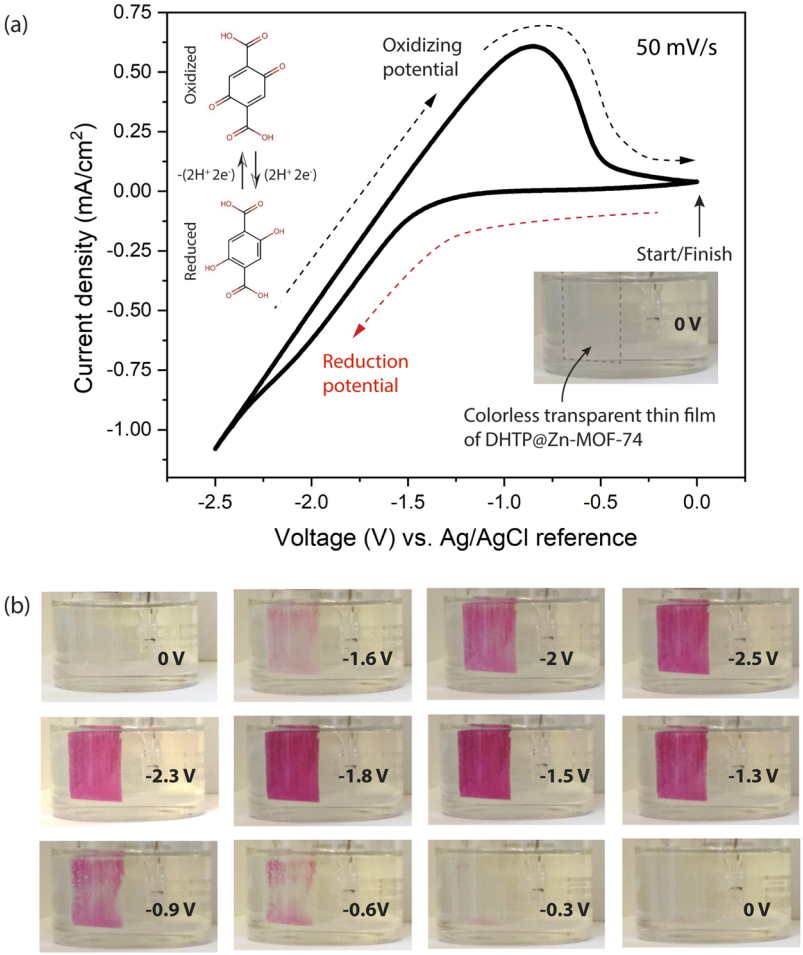

FIG. 3. (a) A representative cyclic voltammetry (CV) curve of the DHTP@Zn-MOF-74 thin film tested in a three-electrode electrochemical cell setup (see Fig. S1 in the supplementary material), by applying a cyclic potential between 0 V and −2.5 V at a scan rate of 50 mV/s. The thin film was subjected to 15 activation cycles under the same test parameters as above before the measurement of this CV curve at cycle No. 20. The inset (top left) shows the possible oxidized and reduced states of the encapsulated DHTP guest molecules. (b) Transformation in the color of the initially transparent thin film of DHTP@MOF-74-Zn on application of a reduction potential from 0 to −2.5 V (first row) followed by an oxidizing potential from −2.5 V to 0 V (second and third rows). The immersed sample area was 2.66 cm^2. Video clips demonstrating color switching in real time during the reduction and oxidation cycles are given in the supplementary material (demo of cycle Nos. 16 and 17 after the activation step).

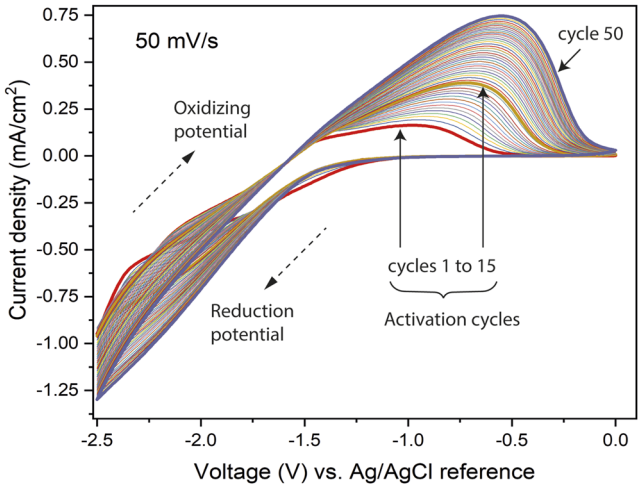

FIG. 4. Evolution of the CV curves of a DHTP@Zn-MOF-74 thin film sample subject to the first 50 cycles at a scan rate of 50 mV/s. The first 15 cycles are marked as activation of the fresh sample. The test was performed up to a maximum of 500 cycles, and the complete cyclic data are presented in Fig. S8 in the supplementary material.

As shown in Fig. 3, when the reduction potential is ramped down from 0 V to −2.5 V, the color of the DHTP@Zn-MOF-74 film (i.e., test electrode) gradually switches from transparent (colorless) to pink and then to light magenta. When the sign of the applied potential is reversed, ramping up from −2.5 V to 0 V under the oxidizing potential, the magenta color of the film becomes increasingly deeper until it reaches an oxidizing potential of about −1.5 V. After surpassing the point corresponding to the maximum current density located at around −0.8 V (i.e., the hump in the CV curve), there is a noticeable reversal of color of the film from magenta to pink, and finally, it turns transparent (colorless) when reaching the neutral state of 0 V. The oxidation potential observed at −0.8 V is reminiscent of the oxidation potential reported in the case of other phenolic compounds,[27] and additionally, in this case, it is unlikely that possible phenoxonium ion at the carbon position where e^- withdrawing -COOH group is situated will form. By looking at the structure of the DHTP molecule, the reversibly forming oxidized and reduced species occur at the 2, 5 positions of DHTP, as depicted in Fig. 3(a) inset.[23,27] It is important to note that the color switch we observed here (colorless ⇄ magenta) is different from that reported for the pristine film of Zn-MOF-74, which switches between the oxidized yellow state ⇄ reduced brown state, requiring a higher voltage of +2 V to −1 V.[28]

The evolution of the CV curves with the number of cycles is shown in Fig. 4. We designate the first 15 cycles as the activation cycles, where the overall shape of the CV curves evolves quite drastically after each cycle. In fact, this is not surprising and occurs when a fresh thin film sample is being exposed to the electrolyte and applied voltage for the first time. During the activation step, we found that the uniformity of the film color gradually improves as the maximum current density rises on completion of each activation cycle. Beyond the activation step and indeed progressing from cycle

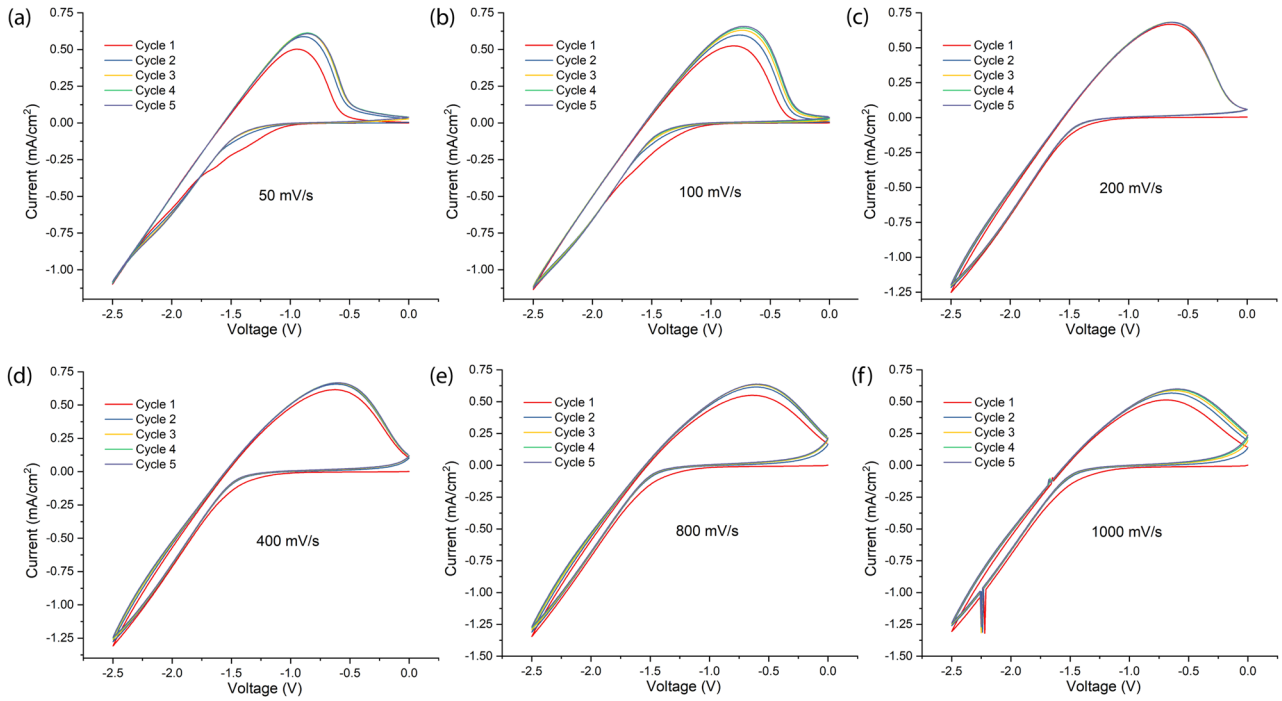

FIG. 5. Cyclic voltammograms of a thin-film sample of Zn-MOF-74 being continuously cycled at an increasingly higher scan rate of (a) 50, (b) 100, (c) 200, (d) 400, (e) 800, and (f) 1000 mV/s. The sample was exposed to 5 cycles per scan rate, thus amounting to 30 cycles in total.

No. 15 up to cycle No. 50, it can be seen in Fig. 4 that the current density in the oxidation test segment continues to rise very systematically. The CV data of the 50-cycle test suggest that the impedance of the film is declining with the rising number of cycles, and this might occur because accessibility to the pore channels of the MOF-74 host is improving with time (No. cycles); it is envisaged that pore channels are not fully accessible to the electrolyte at the beginning of the CV test.

To enable practical applications, it will be of interest to understand the stability and resilience of the electrochromic film when exposed to a much larger number of cycles (to the point when it stops switching color altogether). To address this question, the CV measurements from Fig. 4 were continued up to a maximum of 500 consecutive cycles, maintaining a scan rate of 50 mV/s. The results are presented in Figs. S8(a)–S8(j); we observed that the sample can endure a relatively large number of CV cycles. On the basis of the declining oxidation current density (indicating impedance rise), it can be deduced that material damage becomes prevalent after about 300 cycles, but the film carries on switching its color until the oxidation current density fell to the level of zero evidenced after ~450 cycles. We observed a thick deposition of electrolyte salts on top of the thin film sample after extensive cycling, which prevented us from characterizing the MOF structural integrity.

Finally, the stability of the thin film to color switching at higher scan rates has also been investigated. The results are summarized in Fig. 5. By subjecting the thin film sample to consecutive cycles systematically set at 50, 100, 200, 400, 800, and 1000 mV/s, a good repeatability in CV curves was obtained even at faster switching rates, indicating stable oxidation and reduction cycles of the electroactive DHTP species confined in the channels of MOF-74. In fact, at each scan rate, the data reveal that the redox activity improves gradually with the rising number of cycles.

In summary, this letter presents a facile strategy to spatially confine redox-active guests within the nanoscale MOF pores, hence enabling the fabrication of electrochromic Guest@MOF thin films on a conductive yet mechanically flexible substrate (such as ITO-coated PET for conductivity). This strategy could instigate future electrochromic MOF research, by reinventing conventionally known redox-active species and by leveraging nanoconfined host-guest interactions to derive new properties which are distinct from those of the MOF host or the electroactive guest studied in isolation. Indeed, we recently found that the same methodology can be adopted to fabricate the electrochromic thin film of DHTP@ZIF-8, which is capable of switching between the colorless ⇄ magenta states under an electrical potential of ±4 V (whose results will be presented as a future manuscript). The concept of the electrochromic Guest@MOF film demonstrated in this letter warrants deeper investigations through systematic optical property characterization (e.g., *in situ* UV-Vis absorption/transmittance, coloration efficiency, and switching kinetics) because it has the potential to engineer unconventional material properties beneficial for practical device applications.

See supplementary material for description of the materials' characterization methods, additional SEM and AFM images, PXRD patterns, TGA data, and CV curves of a DHTP@Zn-MOF-74 thin film sample subject to 500 cycles.

We are grateful to the European Union's Horizon 2020 research and innovation program (ERC Consolidator Grant Agreement No. 771575–PROMOFS) and the Samsung GRO Award (No. DFR00230) for supporting this research. We thank Mr Arun Singh Babal for scientific discussions.

REFERENCES

[1] S.-L. Li and Q. Xu, "Metal-organic frameworks as platforms for clean energy," Energy Environ. Sci. **6**(6), 1656–1683 (2013).
[2] A. H. Chughtai, N. Ahmad, H. A. Younus, A. Laypkov, and F. Verpoort, "Metal-organic frameworks: Versatile heterogeneous catalysts for efficient catalytic organic transformations," Chem. Soc. Rev. **44**(19), 6804–6849 (2015).
[3] P. Falcaro, R. Ricco, C. M. Doherty, K. Liang, A. J. Hill, and M. J. Styles, "MOF positioning technology and device fabrication," Chem. Soc. Rev. **43**(16), 5513–5560 (2014).
[4] M. R. Ryder and J. C. Tan, "Nanoporous metal-organic framework materials for smart applications," Mater. Sci. Technol. **30**(13a), 1598–1612 (2014).
[5] I. Stassen, N. Burtch, A. Talin, P. Falcaro, M. Allendorf, and R. Ameloot, "An updated roadmap for the integration of metal-organic frameworks with electronic devices and chemical sensors," Chem. Soc. Rev. **46**(11), 3185–3241 (2017).
[6] S. Kitagawa, R. Kitaura, and S. Noro, "Functional porous coordination polymers," Angew. Chem., Int. Ed. **43**(18), 2334–2375 (2004).
[7] M. D. Allendorf, M. E. Foster, F. Leonard, V. Stavila, P. L. Feng, F. P. Doty, K. Leong, E. Y. Ma, S. R. Johnston, and A. A. Talin, "Guest-induced emergent properties in metal-organic frameworks," J. Phys. Chem. Lett. **6**(7), 1182–1195 (2015).
[8] A. A. Talin, A. Centrone, A. C. Ford, M. E. Foster, V. Stavila, P. Haney, R. A. Kinney, V. Szalai, F. El Gabaly, H. P. Yoon, F. Leonard, and M. D. Allendorf, "Tunable electrical conductivity in metal-organic framework thin-film devices," Science **343**(6166), 66–69 (2014).
[9] K. Leong, M. E. Foster, B. M. Wong, E. D. Spoerke, D. Van Gough, J. C. Deaton, and M. D. Allendorf, "Energy and charge transfer by donor–acceptor pairs confined in a metal–organic framework: A spectroscopic and computational investigation," J. Mater. Chem. A **2**(10), 3389 (2014).
[10] A. K. Chaudhari and J. C. Tan, "Mechanochromic MOF nanoplates: Spatial molecular isolation of light-emitting guests in a sodalite framework structure," Nanoscale **10**(8), 3953–3960 (2018).
[11] A. K. Chaudhari, H. J. Kim, I. Han, and J. C. Tan, "Optochemically responsive 2D nanosheets of a 3D metal-organic framework material," Adv. Mater. **29**(27), 1701463 (2017).
[12] M. K. Carpenter, R. S. Conell, and S. J. Simko, "Electrochemistry and electrochromism of vanadium hexacyanoferrate," Inorg. Chem. **29**(4), 845–850 (1990).
[13] K.-C. Chen, C.-Y. Hsu, C.-W. Hu, and K.-C. Ho, "A complementary electrochromic device based on Prussian blue and poly(ProDOT-Et_2) with high contrast and high coloration efficiency," Sol. Energy Mater. Sol. Cells **95**(8), 2238–2245 (2011).
[14] A. Azam, J. Kim, J. Park, T. G. Novak, A. P. Tiwari, S. H. Song, B. Kim, and S. Jeon, "Two-dimensional WO_3 nanosheets chemically converted from layered WS_2 for high-performance electrochromic devices," Nano Lett. **18**(9), 5646–5651 (2018).
[15] J. Chu, Z. Z. Kong, D. Y. Lu, W. L. Zhang, X. S. Wang, Y. F. Yu, S. Li, X. Q. Wang, S. X. Xiong, and J. Ma, "Hydrothermal synthesis of vanadium oxide nanorods and their electrochromic performance," Mater. Lett. **166**, 179–182 (2016).
[16] K. Kanazawa, K. Nakamura, and N. Kobayashi, "Electroswitchable optical device enabling both luminescence and coloration control consisted of fluoran dye and 1,4-benzoquinone," Sol. Energy Mater. Sol. Cells **145**, 42–53 (2016).
[17] L. Y. Cao, C. Gong, and J. P. Yang, "A solution-processable (tetraaniline-b-polyethylene glycol)(3) star-shaped rod-coil block copolymer with enhanced electrochromic properties," Macromol. Rapid Commun. **37**(4), 343–350 (2016).
[18] S. H. Hsiao and J. Y. Lin, "Electrosynthesis of ambipolar electrochromic polymer films from anthraquinone-triarylamine hybrids," J. Polym. Sci., Part A: Polym. Chem. **54**(5), 644–655 (2016).

[19]C. R. Wade, M. Li, and M. Dinca, "Facile deposition of multicolored electrochromic metal-organic framework thin films," Angew. Chem., Int. Ed. **52**(50), 13377–13381 (2013).
[20]Y.-X. Xie, W.-N. Zhao, G.-C. Li, P.-F. Liu, and L. Han, "A naphthalenediimide-based metal–organic framework and thin film exhibiting photochromic and electrochromic properties," Inorg. Chem. **55**(2), 549–551 (2015).
[21]K. AlKaabi, C. R. Wade, and M. Dincă, "Transparent-to-dark electrochromic behavior in naphthalene-diimide-based mesoporous MOF-74 analogs," Chem **1**(2), 264–272 (2016).
[22]C.-W. Kung, T. C. Wang, J. E. Mondloch, D. Fairen-Jimenez, D. M. Gardner, W. Bury, J. M. Klingsporn, J. C. Barnes, R. Van Duyne, J. F. Stoddart, M. R. Wasielewski, O. K. Farha, and J. T. Hupp, "Metal–organic framework thin films composed of free-standing acicular nanorods exhibiting reversible electrochromism," Chem. Mater. **25**(24), 5012–5017 (2013).
[23]D. Zhang, J. Zhang, H. Shi, X. Guo, Y. Guo, R. Zhang, and B. Yuan, "Redox-active microsized metal-organic framework for efficient nonenzymatic H_2O_2 sensing," Sens. Actuators, B **221**, 224–229 (2015).
[24]S. Mukherjee, B. Manna, A. V. Desai, Y. Yin, R. Krishna, R. Babarao, and S. K. Ghosh, "Harnessing Lewis acidic open metal sites of metal-organic frameworks: The foremost route to achieve highly selective benzene sorption over cyclohexane," Chem. Commun. **52**(53), 8215–8218 (2016).
[25]D. Britt, H. Furukawa, B. Wang, T. G. Glover, and O. M. Yaghi, "Highly efficient separation of carbon dioxide by a metal-organic framework replete with open metal sites," Proc. Natl. Acad. Sci. U. S. A. **106**(49), 20637–20640 (2009).
[26]B. H. Juarez and C. Alonso, "Formation of nanocrystalline zinc on ITO and silicon substrates by electrochemical deposition," J. Appl. Electrochem. **36**(4), 499–505 (2006).
[27]A. Simic, D. Manojlovic, D. Segan, and M. Todorovic, "Electrochemical behavior and antioxidant and prooxidant activity of natural phenolics," Molecules **12**(10), 2327–2340 (2007).
[28]I. Mjejri, C. M. Doherty, M. Rubio-Martinez, G. L. Drisko, and A. Rougier, "Double-sided electrochromic device based on metal-organic frameworks," ACS Appl. Mater. Interfaces **9**(46), 39930–39934 (2017).